Eur. Phys. J. B **12**, 217–223 (1999)

THE EUROPEAN PHYSICAL JOURNAL B

EDP Sciences

Double-exchange model: phase separation versus canted spins

M.Yu. Kagan[1], D.I. Khomskii[2,a], and M.V. Mostovoy[2]

[1] P.L. Kapitza Institute for Physical Problems, Kosygina Street 2, 117334 Moscow, Russia
[2] University of Groningen, Nijenborgh 4, 9747 AG, Groningen, The Netherlands

Received 17 March 1999

Abstract. We study the competition between different possible ground states of the double-exchange model with strong ferromagnetic exchange interaction between itinerant electrons and local spins. Both for classical and quantum treatment of the local spins the homogeneous canted state is shown to be unstable against a phase separation. The conditions for the phase separation into the mixture of the antiferromagnetic and ferromagnetic/canted states are given. We also discuss another possible realization of the phase-separated state: ferromagnetic polarons embedded into an antiferromagnetic surrounding. The general picture of a percolated state, which emerges from these considerations, is discussed and compared with results of recent experiments on doped manganaties.

PACS. 75.10.-b General theory and models of magnetic ordering – 75.30.Mb Valence fluctuation, Kondo lattice, and heavy-fermion phenomena – 75.30.Kz Magnetic phase boundaries (including magnetic transitions, metamagnetism, etc.)

1 Introduction

The double-exchange model describing itinerant electrons interacting with local spins was first used to explain ferromagnetism in metals, such as Ni and Fe [1]. The revival of interest to this model was prompted by the recent observation of the colossal magnetoresistance (CMR) in manganites [2]. The limit of strong ferromagnetic (FM) exchange between the conducting electrons and spins, relevant for manganites, was first discussed by de Gennes [3]. He suggested that the competition between the antiferromagnetic (AFM) superexchange and the double exchange results in the canting of the AFM state (the angle θ between the spins from different sublattices becomes smaller than π). The canting angle grows with the concentration of charge carriers, which explains the increase of magnetization upon doping observed in $La_{1-x}Ca_xMnO_3$.

However, already rather long ago arguments against the canted ground state were put forward, most notably by Nagaev [6]. In the de Gennes approach the local spins were treated classically. Quantum corrections stabilize the AF state and the canting appears only above certain concentration of charge carriers [6].

A more fundamental problem is that at partial filling of the conduction band any homogeneous ground state may be unstable against a phase separation. Such an instability takes place in the Hubbard model away from half-filling [4] and in the t-J model [5]. In a wide range of parameters the ground state of these models is phase-separated, stable homogeneous solutions being rather an exception. In this respect the double-exchange model is rather similar, which can be seen already from the tendency to a formation of magnetic polarons in this model [6,7]. These polarons are FM droplets surrounding charge carriers in the AF background. If for some reason (large effective mass, disorder) the polarons become immobile, they can be viewed as a form of the FM-AFM phase separation (see also [8,9]).

The phase separation in the double-exchange model would imply that many experimental data on doped manganites should be reinterpreted taking into account the magnetic and electronic inhomogeneity of the ground state. In particular, the charge transport and the metal-insulator transition should be described in terms of percolation rather than by the properties of some pure states. The percolation in managanites was emphasized by Gorkov and Kresin in reference [10]. Some recent experimental results also strongly point in this direction [11–13].

In this paper we discuss the instability against the phase separation in the double-exchange model. Although we mostly keep in mind applications to CMR manganites, our treatment has a general character. We go beyond the classical treatment of local spins used in most numerical studies of the double-exchange model. Our treatment has some points in common with the previous investigations. Nevertheless, we think it is worthwhile to include (with necessary modifications) some old results, so as to have a full coherent picture of the behavior of this system.

Our paper is organized as follows. After formulating the model in Section 2, we discuss the homogeneous canted state, taking into account quantum effects. Several critical

[a] e-mail: khomskii@phys.rug.nl

concentrations separating different regimes are identified. In Section 3 we demonstrate that for small concentrations of charge carriers the homogeneous canted state is unstable against a phase separation. In Section 4 the general phase diagram of the double-exchange model is discussed. The Maxwell construction is used to investigate the characteristics of the coexisting phases. It is shown, in particular, that depending on the parameters, there may be phase separation not only on AFM and FM phases, but also on AFM and canted states. Then in Section 5, we consider the polaronic state and explicitely show that the energy of this inhomogeneous state is lower than the energy of the homogeneous canted state, even when quantum effects are taken into account. Finally, in the concluding Section 6 we summarize the main results and discuss the resulting picture in relation to some recent experimental observations.

2 Energy of homogeneous canted state

We consider the double-exchange Hamiltonian describing the interaction of itinerant electrons with localized spins, to which we add the Heisenberg interaction between the spins (FM Kondo-lattice model):

$$H = -t\sum_{\langle ij\rangle\sigma}\left(c^{\dagger}_{i\sigma}c_{j\sigma}+c^{\dagger}_{j\sigma}c_{i\sigma}\right)-J_{\rm H}\sum_{i}\mathbf{S}_i\mathbf{s}_i + J\sum_{\langle ij\rangle}\mathbf{S}_i\mathbf{S}_j. \quad (1)$$

Here, the first term describes the hopping of conduction electrons, the second term is the on-site FM exchange between the spin of a conduction electron $\mathbf{s}$ and the localized spin $\mathbf{S}$, and the last term is the AFM exchange between the nearest localized spins ($J_{\rm H}, J > 0$). We assume the value of localized spins to be large: $S \gg 1$. Furthermore, we consider the case of strong Hund coupling $J_{\rm H}$ and weak Heisenberg coupling J:

$$J_{\rm H}S \gg t \gg JS^2. \quad (2)$$

Finally, in this paper we consider the simple cubic lattice.

The model (1) describes the competition between the direct antiferromagnetic exchange of the localized spins and the double exchange *via* the conduction electrons, which tends to order the spins ferromagnetically. The simplest state that could result from this competition, is a canted state, which has the features of both the FM and AFM states: as in the AFM state, the localized spins in the canted state form two sublattices, however an angle θ between the magnetizations of the sublattices is, in general, arbitrary, so that the total magnetic momentum of the system is nonzero. The canted state interpolates between the AFM state ($\theta = \pi$) and the FM state ($\theta = 0$).

In the classical treatment of localized spins, used in reference [3], the orientation of the spins is fixed:

$$\mathbf{S}_i = \begin{cases} S\mathbf{n}_{\rm A} \text{ if } i \in {\rm A} \\ S\mathbf{n}_{\rm B} \text{ if } i \in {\rm B} \end{cases}, \quad (3)$$

where A and B denote the two sublattices and the unit vectors $\mathbf{n}_{\rm A}$ and $\mathbf{n}_{\rm B}$ describe the direction of the magnetization of the corresponding sublattice. Such a state we shall call the classical canted (CC) state.

In another approach [6], one assumes that equation (3) only holds on sites that are not occupied by conduction electrons. In the quantum language, the localized spins on empty sites have the maximal projection, $+S$, on the magnetization vector of the corresponding sublattice. On occupied sites, however, the localized spin $\mathbf{S}$ and the spin of a conduction electron $\mathbf{s}$ form a state with the maximal total spin $S_{\rm tot} = S + \frac{1}{2}$, because it has the lowest energy in the large-$J_{\rm H}$ limit. The projection of the total spin on the axis of the corresponding sublattice can have only two values: $S^z_{\rm tot} = S \pm \frac{1}{2}$ (otherwise, the localized spin cannot remain in the state with the maximal projection after the conduction electron leaves the site). The hopping of electrons between the two sublattices is then described by a 2×2 matrix. Diagonalizing this matrix one obtains two electron bands with the corresponding hopping amplitudes [6],

$$t_{\pm} = t\left[\frac{\sqrt{2S+1+S^2\cos^2\frac{\theta}{2}}}{2S+1} \pm \frac{S\cos\frac{\theta}{2}}{(2S+1)}\right] = \frac{t}{\sqrt{2S+1}}{\rm e}^{\pm\gamma}, \quad (4)$$

where γ is defined by $\sinh\gamma = S\cos\frac{\theta}{2}/\sqrt{2S+1}$. The two-band canted state is referred below as the quantum canted (QC) state (though the quantum fluctuations of local spins are not taken into account in this approach).

The origin of the two hopping amplitudes $t_{\pm}$ can be easily understood on the simple examples. For the AFM state ($\theta = \pi$) the two bands have the same width: $t_+ = t_- = \frac{t}{\sqrt{2S+1}}$. An electron, propagating coherently in the AFM spin background, creates a state with $S^z_{\rm tot} = S + \frac{1}{2}$ on one sublattice and a state with $S^z_{\rm tot} = S - \frac{1}{2}$ on the other:

$$\left|S^z_{\rm tot} = S+\frac{1}{2}\right\rangle \rightarrow \left|S^z_{\rm tot} = S-\frac{1}{2}\right\rangle \rightarrow \left|S^z_{\rm tot} = S+\frac{1}{2}\right\rangle \ldots,$$

which closely resembles a type of motion considered by Zaanen *et al.* in reference [14]. Similarly, for the FM ordering ($\theta = 0$) we obtain from (4) $t_+ = t$ and $t_- = \frac{t}{2S+1}$. Here, t_+ corresponds to the motion of a spin-up electron in the spin-up FM background, whereas t_- describes the motion of the spin-down electron in the same background. In the latter case, on each site the electron spin and the local spin form the $|S^z_{\rm tot} = S - \frac{1}{2}\rangle$ state.

We denote by $n_{\pm}$ the densities of electrons occupying the two bands, so that

$$n_+ + n_- = n, \quad (5)$$

where n is the total electron density. As we shall shortly see, under condition (2) the transitions between the AFM, canted, and FM states take place at $n \ll 1$. In this case

all occupied electron states lie close to the bottom of each of the two bands, and the momentum dependence of the electron energy can be approximated by:

$$\varepsilon_{\pm}(\mathbf{p}) = -zt_{\pm} + \frac{p^2}{2m_{\pm}},$$

where $\frac{1}{2m_{\pm}} = t_{\pm}$ (the lattice constant is put to 1) and $z = 6$ is the number of nearest neighbors. The densities $n_{\pm}$ are related to the corresponding Fermi momenta $p_{\mathrm{F}\pm}$ by

$$n_{\pm} = \frac{p_{\mathrm{F}\pm}^3}{6\pi^2}, \tag{6}$$

and the chemical potential of conducting electrons is:

$$\mu = -zt_{+} + \frac{p_{\mathrm{F}+}^2}{2m_{+}} = -zt_{-} + \frac{p_{\mathrm{F}-}^2}{2m_{-}}. \tag{7}$$

The second part of equation (7) only holds if both electron bands are occupied.

The energy (per site) can then be written as follows:

$$E = \frac{z}{2}JS^2\cos\theta - zt_{+}n_{+} - zt_{-}n_{-} + at_{+}n_{+}^{5/3} + at_{-}n_{-}^{5/3}, \tag{8}$$

where the first term is the energy of the AFM exchange between localized spins and other terms represent the energy of conducting electrons ($a = \frac{3}{5}(6\pi^2)^{2/3}$).

The large energy of the on-site FM exchange, $-J_{\mathrm{H}}\frac{S}{2}n$, is substracted from equation (8), as it only renormalizes the chemical potential. For $n \ll 1$, the fourth and fifth terms in equation (8) (the kinetic energy of electrons counted from the bottom of the corresponding band) are small compared to, respectively, the second and the third terms. Therefore, in this section the last two terms will be neglected (their role is considered in Sect. 3).

We first consider the case when the canting angle θ is very close to π and $\gamma \ll 1$, so that, according to equation (4), the difference between t_{+} and t_{-} is relatively small and the two electron bands are filled almost equally: $(n_{+} - n_{-})/n_{+} \ll 1$. Then, using equations (4, 7), the energy of the QC state is approximately:

$$E_{\mathrm{QC}} = -\frac{tzn}{\sqrt{2S+1}} - \frac{z}{2}JS^2 + \frac{z}{3}J(2S+1)\left[-\frac{(n-n_1)}{n_1}\gamma^2 + \frac{z^6t^4}{32\pi^8(2S+1)J^4}\gamma^4\right], \tag{9}$$

where

$$n_1 = \frac{8\pi^4}{3}\left(\frac{J(2S+1)^{3/2}}{zt}\right)^3. \tag{10}$$

The optimal value of γ can be found from the condition $\mathrm{d}E/\mathrm{d}\gamma^2 = 0$ and is given by:

$$\gamma^2 = \begin{cases} 0 & \text{for } n < n_1 \\ \dfrac{6\pi^4 J(2S+1)^{3/2}}{z^3 t}(n-n_1) & \text{for } n > n_1 \end{cases} \tag{11}$$

(the last expression is only valid for $(n - n_1)/n_1 \ll 1$).

While in the classical treatment of de Gennes the canting of sublattices takes place at arbitrarily small doping [3], in the quantum treatment the system stays antiferromagnetic up to the critical concentration n_1 [6]. This happens because in the two-band picture electrons can propagate even in the colinear AFM state *via* the process described above, while in the classical treatment they are localized. The two bands have the same width, $\frac{2zt}{\sqrt{2S+1}}$, and are equally occupied, so that the energy of the AFM state is:

$$E_{\mathrm{AFM}} = -\frac{tzn}{\sqrt{2S+1}} - \frac{z}{2}JS^2. \tag{12}$$

For $n > n_1$, the energy of the two-band QC state becomes lower than the energy of the AFM state:

$$E_{\mathrm{QC}} = E_{\mathrm{AFM}} - \frac{3}{8}\frac{zt^2}{J(2S+1)^2}(n-n_1)^2. \tag{13}$$

As γ grows with increasing n, so does the difference between t_{+} and t_{-}. As a result, above certain concentration n_2 the second part of equation (7) can no longer be satisfied. Thus, for $n > n_2$ only the "+" band is filled, while the "−" band is empty ($n_{+} = n$ and $n_{-} = 0$).

The energy of the one-band QC state is given by

$$E_{\mathrm{QC}} = -zt_{+}n - \frac{z}{2}JS^2 + zJ(2S+1)\sinh^2\gamma. \tag{14}$$

An optimal value of γ for $n > n_2$ satisfies

$$\mathrm{e}^{-\gamma}\sinh 2\gamma = \frac{nt}{J(2S+1)^{3/2}}. \tag{15}$$

The concentration n_2, at which the second band disappears, is found using equation (15) and

$$z(t_{+} - t_{-}) = \frac{p_{\mathrm{F}}^2}{2m_{+}} = t_{+}n_2^{2/3}$$

(*cf.* Eq. (7)) to be

$$n_2 \approx \frac{27}{2}n_1. \tag{16}$$

When γ becomes much larger than 1, the hopping amplitude $t_{+} \approx t\cos\frac{\theta}{2}$, *i.e.*, it coincides with the classical expression used by de Gennes. In this case we recover the CC state with the energy

$$E_{\mathrm{CC}} = -ztn\cos\frac{\theta}{2} + \frac{z}{2}JS^2\cos\theta. \tag{17}$$

The optimal canting angle is given by $\cos\frac{\theta}{2} = \frac{tn}{2JS^2}$, so that the optimal energy of the CC state (for $S \gg 1$) is

$$E_{\mathrm{CC}} = -\frac{zt^2n^2}{4JS^2} - \frac{z}{2}JS^2. \tag{18}$$

The cross-over from the one-band QC state to the CC state occurs at

$$n \sim n_3 = \frac{8JS^{3/2}}{t}. \tag{19}$$

Finally, for

$$n > n_4 = \frac{2JS^2}{t}, \tag{20}$$

the angle $\theta = 0$, *i.e.*, the canted state transforms into the FM state with the energy:

$$E_{\rm FM} = -ztn + \frac{z}{2}JS^2. \tag{21}$$

Summarizing the results of these section, we can say that on the class of the homogeneous trial ground states with two sublattices, the AFM state is the most favorable for $n < n_1$. For $n_1 < n < n_2$ the two-band QC state has lower energy. For $n > n_2$ only one of the bands is filled. For $n \gtrsim n_3$ the one-band QC state coincides with the CC state. Finally, for $n > n_4$ the ground state is ferromagnetic.

3 Instability of canted state against phase separation

In this section we study the stability of the canted state against a phase separation by calculating the electronic compressibility,

$$\kappa^{-1} = \frac{{\rm d}^2E}{{\rm d}n^2}.$$

It is easy to see that under the condition (2) and for small n the compressibility is negative. Thus, for the two-band QC state at $n \gtrsim n_1$

$$\kappa^{-1} = -\frac{3}{4}\frac{zt^2}{J(2S+1)^2}, \tag{22}$$

(*cf.* Eq. (13)), while in the classical canted regime (see Eq. (17))

$$\kappa^{-1} = -\frac{zt^2}{2JS^2}. \tag{23}$$

We see, therefore, that the homogeneous canted (both classical and quantum) state is unstable for small n. This instability is similar to the instability against a phase separation in the Hubbard model [4] and t-J model [5].

At sufficiently large n the kinetic electron energy makes the compressibility of the canted state positive. For arbitrary band-filling equation (17) for the energy of the CC state has to be substituted by

$$E_{\rm CC}(n) = -t\cos\frac{\theta}{2}f(n) - \frac{\bar{J}}{2}\cos\theta, \tag{24}$$

where $f(n)$ is the kinetic energy of electrons with the hopping amplitude $t = 1$ (which depends only on the electron density n), and $\bar{J} = zJS^2$. Then the canting angle is given by

$$\cos\frac{\theta}{2} = \frac{tf(n)}{2\bar{J}} \tag{25}$$

and the energy of the CC state is

$$E_{\rm CC}(n) = -\frac{t^2}{4\bar{J}}f(n)^2 - \frac{\bar{J}}{2}. \tag{26}$$

For small band-filling $f(n) \approx -zn$ and the last equation agrees with equation (18). While for small n the compressibility is negative, the increase of the electron density results in the increase of the Fermi-pressure of the electron gas, which stabilizes the canted state. At half-filling the electron energy, $f(n)$, reaches minimum and, according to equation (26), so does the energy of the CC state. Thus, at least close to half-filling $\kappa > 0$. For $D = 3$, the compressibility of the CC state is positive for $n \gtrsim 0.16$.

4 Phase diagram

In this section we discuss the phase diagram of the double-exchange model. We treat spins classically ($S \to \infty$), keeping, however, $\bar{J} = zJS^2$ finite (the numerical calculations in this section were performed for $D = 3$, but the behavior in other dimensions is qualitatively the same). In Figure 1 we plot the energy of a homogeneous state, $E(n)$, which is the CC state, for $n < n_4$, and the FM state for $n > n_4$. The energy of the CC state is given by equation (26), while the energy of the FM state for arbitrary density is

$$E_{\rm FM}(n) = tf(n) + \frac{\bar{J}}{2}.$$

For small n, the CC state separates on the pure AFM phase and a second phase that contains all the electrons. The density of electrons in the second phase, n_*, is defined by the Maxwell construction:

$$\frac{{\rm d}E(n_*)}{{\rm d}n_*} = \frac{E(n_*) + \frac{1}{2}\bar{J}}{n_*}. \tag{27}$$

For $n_* > n_4$, the second phase is ferromagnetic (see Fig. 1a), while for $n_* < n_4$ it is the stable canted state (see Fig. 1b). Which of the two situations is realized depends on the ratio of $\bar{J}/t$. For the small ratio ($\bar{J}/t <\sim 0.425$ in 3D), the phase separation goes into the pure AFM and FM states, for larger $\bar{J}/t$, the ground state is the mixture of the AFM and stable canted states. This is illustrated in Figure 2, where we plot the phase diagram of the system. The thick line shows the dependence of n_* on $\bar{J}/t$ and separates stable states from unstable states. In the ferromagnetic region of the diagram n_* grows with $\bar{J}/t$, while in the canted region $n_* \approx 0.291$ independent of $\bar{J}/t$ (both sides of Eq. (27) with $E = E_{\rm CC}$ can be divided by $t^2/\bar{J}$, after which the equation becomes independent of t and $\bar{J}$). In the unstable FM region and a part of the unstable canted region the compressibility is positive, so that the corresponding states are locally stable. They are, however, globally unstable against the phase separation, as follows form the Maxwell construction.

In the $J_{\rm H} \gg t$ and $S \gg 1$ limit, we consider in this section, the phase diagram of the double-exchange model is symmetric around $n = 1/2$. This can be seen by applying to the Hamiltonian (1) the particle-hole transformation

$$c_i \to \begin{cases} +h_i^\dagger \text{ for } i \in \text{A} \\ \\ -h_i^\dagger \text{ for } i \in \text{B} \end{cases},$$

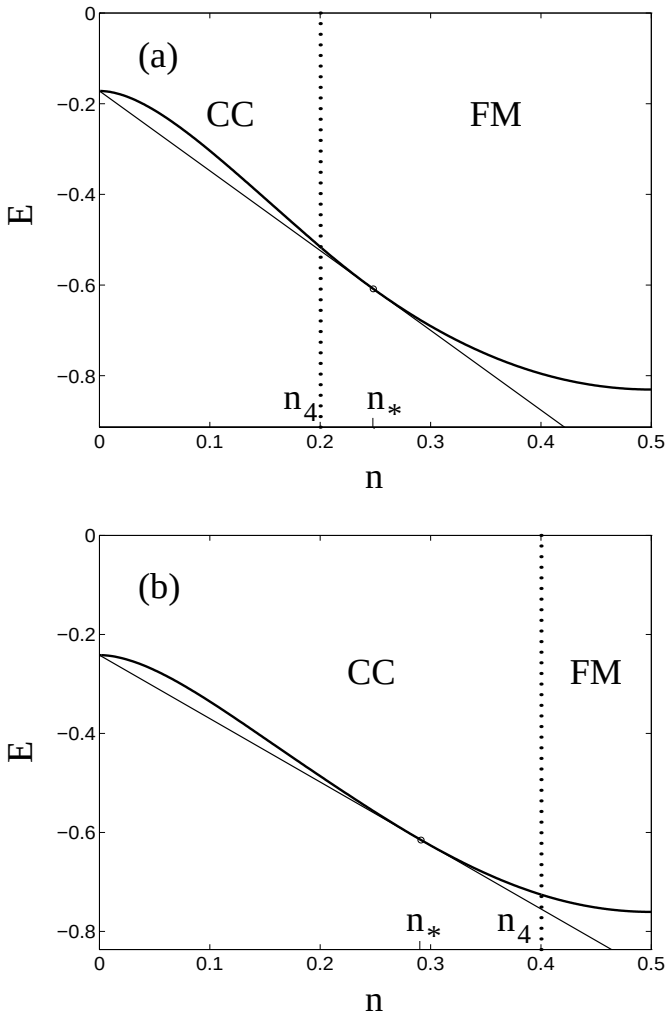

Fig. 1. The energy of a homogeneous state E as a function of electron density n (thick line) calculated for two different values of $\bar{J}/t$: ~ 0.344, corresponding to $n_4 = 0.2$, (a) and ~ 0.484, corresponding to $n_4 = 0.4$. The Maxwell construction (thin line) gives the density n_* of the phase containing all the electrons in the phase-separated state. For $n_4 < n_*$, the phase-separated state is the mixture of the AFM and FM states (a), while for $n_4 > n_*$ it is the mixture of the AFM and CC states (b).

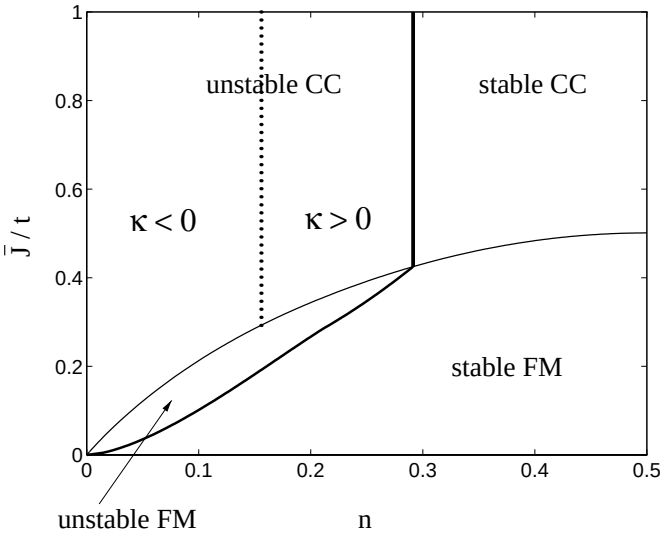

Fig. 2. The phase diagram of the double-exchange model. The states to the left of the thick line are unstable against the phase separation. The thick line shows the dependence of the density n_* of the electron-reach phase on J/t. The thin line separates the canted state from the ferromagnetic state. The regions of the CC state with positive and negative compressibility are separated by the dotted line.

where c_i annihilates electron on site i with spin parallel to the local spin on the same site, while h_i is a corresponding hole operator. This transformation leaves the kinetic energy term (first term in (1)) unchanged, but it reverses the sign of the Hund's coupling (the second term in (1)). The fact that holes are coupled to local spins antiferromagnetically, rather than ferromagnetically, does not, however, make any difference: the important thing is that the orientation of the spin of the hole is uniquely determined by the orientation of the local spin. Thus, the double-exchange system with n holes per site (*e.g.*, with electron density $1-n$) has the same properties as the system with n electrons per site.

Experimentally, however, there is a marked difference in the behavior of the hole-doped manganites ($La_{1-x}M_xMnO_3$, M = Sr, Ca, $x < 0.5$) and the electron-doped (overdoped) manganites ($x > 0.5$, the electron density related to doping by $n = 1 - x$). While the properties of the hole-doped systems qualitatively resemble those described above, the electron-doped manganites (with predominantly Mn^{4+}) behave quite differently: they are mostly insulating, often with charge ordering in the form of stripes [15] and sometimes with anisotropic magnetic structures [16]. The reason for the asymmetry of the phase diagram is not completely clear. One of the factors, which is not taken into account in the double-exchange model studied above, but which may play an important role, is the orbital degeneracy of the electrons bands [17]. Note, however, that the tendency to a phase separation discussed in this paper is also present for the degenerate bands [17].

5 Polaron state

There exist many different realizations of an inhomogeneous phase-separated state. For the model (1) the most favorable one is the complete phase separation (considered in the previous section), in which case one part of the sample contains all the charge carriers and is ferromagnetic (or strongly canted), while the other part is an undoped antiferromagnet. Such a phase separation would, however, be counteracted by the Coulomb interaction (not included in the Hamiltonian (1)). The Coulomb interaction may suppress the phase separation completely, or it could favor the formation of the FM droplets (spin-bags) immersed

into the AFM matrix. More complicated structures, *e.g.*, stripes [18] are also possible. In general, the phase separation in the double-exchange model in the presence of Coulomb interactions seems to be rather similar to that in the t-J model considered in the context of the high-T_c superconductors [5,18]. In the later case, the instability towards the phase separation remains even with the Coulomb interaction taken into account.

In this section we consider a simple type of the phase separated state: the AFM matrix with the FM "droplets", each containing one electron. In other words, we assume that electrons propagating in the AFM background form ferromagnetic polarons [6,7]. Such a state, with only one electron per droplet and with the droplets well separated from each other will help to minimize the Coulomb energy contribution mentioned above. We will demonstrate that the energy of this state is, indeed, lower than that of the homogeneous canted state.

We calculate now the energy of the system for small doping, $n \ll 1$, assuming that each electron is localized inside a FM sphere of radius R. The energy of such a state can is given by

$$E_{\rm P} = - - tn\left(z - \frac{\pi^2}{R^2}\right) + n\frac{\bar{J}}{2}\frac{4}{3}\pi R^3 - \frac{\bar{J}}{2}\left(1 - n\frac{4}{3}\pi R^3\right). \tag{28}$$

The first term in (28) is the energy of the lowest state of an electron in the sphere, while the second and the third terms give, respectively, the exchange energy of localized spins in the ferromagnetic regions and in the remaining antiferromagnetic matrix. The ferromagnetic polarons are assumed to have sharp boundaries and the surface energy is neglected. Furthermore, we assume that the polarons do not overlap, in which case the change of the energy of the system due to doping is simply proportional to n.

The optimal polaron radius, found from the condition $\mathrm{d}E_{\rm P}/\mathrm{d}R = 0$, is given by

$$R = \left(\frac{\pi t}{2\bar{J}}\right)^{1/5} \tag{29}$$

and the energy of the polaron state is:

$$E_{\rm P} = -\frac{\bar{J}}{2} - ztn + \frac{5\pi}{3}n(\pi t)^{3/5}(2\bar{J})^{2/5}. \tag{30}$$

It is easy to see that the energy of such a polaron state is lower than the energy of both the classical and the quantum homogeneous canted states. Moreover, at $n = n_4$ the polaron state is also more favorable than the FM state. Only at higher concentration,

$$\frac{3}{10\pi}\left(\frac{2\bar{J}}{\pi t}\right)^{3/5},$$

the transition to the saturated FM state occurs. At this concentration polarons begin to overlap and for small $\bar{J}/t$ this concentration up to a numerical factor coincides with n_* discussed in the previous section.

As the magnetic polarons can move, the polaronic state is, in principle, homogeneous. However, in the limit $\bar{J} \ll t$, mainly discussed in this paper, the magnetic polarons are large (see Eq. (29)), their mobility is low and they are easily localized by disorder and Coulomb interactions. Thus, the polaronic state with large polarons can be considered as a special form of a phase-separated state.

Ferromagnetic polarons can be also formed in materials with layered electronic and magnetic structure, such as manganites. In $LaMnO_3$ the layers are formed by planes of ferromagnetically coupled localized spins, while the exchange between the spins from two neighboring layers is antiferromagnetic. Also, the interlayer and intralyer hopping amplitudes, $t_\parallel$ and $t_\perp$, are different. Such a layered magnetic and electronic structure is a result of the orbital ordering that takes place in this material [19]. The polaron is elongated ("cucumber") for $t_\parallel > t_\perp$ and compressed ("pancake") for $t_\parallel < t_\perp$. A detailed discussion of the FM polaron in the layered system will be given elsewhere.

6 Conclusions

In conclusion, we have shown that the tendency to a phase separation and a formation of a spatially inhomogeneous state, found for several models of strongly correlated electrons, is also an inherent property of the double-exchange model. For large Hund's coupling, $J_{\rm H} \gg t \gg JS^2$, and small doping the homogeneous canted state has negative compressibility. This is related to the instability of the canted state against the phase separation into pure antiferromagnetic and ferromagnetic phases. The latter phase contains all charge carriers. For $zJS^2 \sim t$ the compressibility of the canted state is negative only at small concentrations of charge carriers. In that case, it can separate into the pure antiferromagnetic phase and the canted state with a large concentration of charge carriers and a large canting angle.

The spatially inhomogeneous state may occur in a variety of different forms, *e.g.*, a random mixture of AFM and FM phases, magnetic polarons ("fog" of small FM droplets), or some regular structure, such as stripes. Which of this situations is realized would depend on specific conditions and may be different in different parts of the phase diagram. However, the tendency to form an inhomogeneous state seems to be a generic property of the double-exchange model. The specific features of manganaties (layered magnetic structure, orbital degeneracy), though definitely important for determining a particular form of the ground state, nevertheless seem to preserve this tendency.

Several theoretical problems still remain to be clarified. The first one, already mentioned above, is the role of the Coulomb interaction in determining a detailed nature of the inhomogeneous state (the average size of polarons and their spatial ordering (*cf.* experimental results [20])). Another question is the detailed spin structure both inside and outside polarons. In the treatment above we made a simplifying assumption that the inner part is the saturated ferromagnet, while the outer part is the pure antiferromagnet without canting. However, in general, this

need not to be the case: both these phases may have certain degree of canting. In particular, since the spectrum of spin excitations in AF matrix is gapless, the distortion of the perfect antiferromagnetic order should decay slowly with the distance from a polaron [3]. All these questions definitely require further study, but at this point we can, in any case, say that the homogeneous canted state seems to be nearly always unstable, and inhomogeneous structures of some kind have to be realized in low-doped double exchange systems, including CMR manganites.

Turning to an experimental situation in manganites, we can state that there exist already many indications that the phase separation is indeed present there. The formation of stripe phases in overdoped $La_{1-x}Ca_xMnO_3$ ($x > 0.5$) [15] can be viewed as a manifestation of this tendency. However, much more indications of this are now observed in the most interesting region of $x < 0.5$ and, in particular, in the CMR regime. Already the old data [21] on a coexistence of both the FM and AFM phases in the magnetic neutron scattering, which are sometimes treated in a picture of homogeneous canted state, are actually much better interpreted as a mixture of FM and AFM microregions [6]. Recent neutron scattering results [20] confirm this picture and, moreover, show the presence of spatial liquid-like correlations of the FM droplets (in the system studied in [20] these were not purely FM droplets, but rather the microregions with the large canting angle). Direct confirmation of the existence of the inhomogeneous state comes from the NMR measurements [12], which show the presence of two different hyperfine fields corresponding to FM and AFM regions. And finally, quite recently the presence of an inhomogeneous state with a random mixture of phases with different electronic properties, was directly visualized by the STM study of $La_{0.7}Ca_{0.3}MnO_3$ [22]: the metallic and insulating regions with an average scale of 10-50 nm were directly seen in this investigation.

The natural consequence of the phase separation is that the main properties of CMR manganites, including transport properties, should be treated in the percolation picture [10]. This concept explains quite naturally the critical doping $x_c \sim 0.16$, above which the ferromagnetic metallic state appears in $La_{1-x}M_x^{2+}MnO_3$ [10]. An experimental support for the percolation picture comes from the recent study [13], which shows that $I - V$ characteristics of $La_{1-x}Pr_xCa_{0.3}MnO_3$ are strongly nonlinear even at small voltages: such behavior is expected for the percolated state, for which the electric field would modify the distribution and shape of metallic clusters and enhance conductivity.

Thus, both from the theoretical treatment and from many experimental results it follows that, most probably, the electronic and magnetic state of doped manganites is intrinsically inhomogeneous, leading to the percolated state. This should be definitely the case for small doping (for which the random potential of impurities should be also taken into account); but it is also quite probable that such is the nature of even optimally doped manganites ($x \sim 0.3$) with CMR. This gradually emerging picture, promisses to give a new explanation of the properties of these fascinating materials.

Authors are greatful to E.L. Nagaev, L.P. Gor'kov, M. Hennion, N.A. Babushkina, K.I. Kugel, R. Ibarra, J.M. Coey, G.A. Sawatzky, J. Aarts, J. Mydosh, P. Guinea and many other collegues for useful discussions and for information of the new experimental results prior to their publication. This work was supported by NWO grant and President Eltsin grant #97-26-15H/363, by the Dutch Foundation for Fundamental Studies of Matter (FOM) grant, and by the Eropean Network OXSEN.

References

1. C.S. Zener, Phys. Rev. **82**, 403 (1951).
2. See, *e.g.*, A.P. Ramirez, J. Phys. Cond. Matter **9**, 8171 (1997).
3. P.G. de Gennes, Phys. Rev. **118**, 141 (1960)
4. P.B. Visscher, Phys. Rev. B **10**, 943 (1974).
5. V.J. Emery, S.A. Kivelson, H.Q. Lin, Phys. Rev. Lett. **64**, 475 (1990).
6. E. L. Nagaev, *Physics of Magnetic Semiconductors* (Moscow, Mir Publ., 1979); Sov. Phys.-Uspekhi **166**, 833 (1996).
7. T. Kasuya, A. Yanase, T. Takeda, Solid State Comm. **8**, 1543 (1970).
8. S. Yunoki, J. Hu, A.L. Malvezzi, A. Moreo, N. Furukawa, E. Dagotto, Phys. Rev. Lett., **80**, 845 (1998).
9. D. Arovas, F. Guinea, Phys. Rev. B **58**, 9150 (1998).
10. L.P. Gorkov, V.Z. Kresin, JETP Lett. **67**, 985 (1998).
11. M. de Teresa *et al.*, Nature (London) **386**, 256 (1997).
12. G. Allodi *et al.* Phys. Rev. B **56**, 6036 (1997).
13. N.A. Babushkina *et al.*, Phys. Rev. B **59**, 6994 (1999).
14. J. Zaanen, A.M. Oles, P. Horsch, Phys. Rev. B **46**, 5798.
15. S. Mori, C.H. Chen, S.-W. Cheong, Nature **392**, 473 (1998).
16. T. Akimoto *et al.*, Phys. Rev. B **57**, R5594 (1997).
17. J. van den Brink, D. Khomskii, Phys. Rev. Lett. **82**, 1016 (1999).
18. J. Zaanen, N.L. Horbach, W. van Saarlos, Phys. Rev. B **53**, 8671 (1996).
19. D.I. Khomskii, G.A. Sawatzky, Solid State Comm. **102**, 87 (1997).
20. M. Hennion *et al.*, Phys. Rev. Lett. **81**, 1957 (1998).
21. E.O. Wollan, W.C. Koeler, Phys. Rev. **100**, 545 (1955).
22. M. Fäth *et al.*, Science **285**, 1540 (1999).